AN ABSTRACT OF THE THESIS OF

Jumpei Baba for the degree of Master of Science
(Name) (Degree)

in Oceanography presented on 27 May 1980
(Major) (Date)

Title: EXPERIMENTS ON THE SETTLING BEHAVIOR OF IRREGULAR GRAINS IN A FLUID

Abstract Approved
Paul D. Komar

The settling behavior of irregular particles were studied in two sets of experiments covering two different ranges of grain sizes. Analyses were made to quantify the grain irregularities such as sphericity and grain roundness. In each study empirical relationships were developed for the prediction of settling velocities of irregular grains.

In the first set of experiments, irregular glass particles collected from Oregon beaches, showing various degrees of roundness, were settled in a tube filled with glycerine, yielding Reynolds numbers equivalent to the settling of silt to very fine quartz sand in water. Each grain was measured for its weight, roundness and sphericity. Grain roundness was determined using Power's scale, and sphericity was defined by Janke's E shape factor. During the experiments, most of the particles showed almost no irregular motions, and settled with their maximum projection areas perpendicular to the fall direction. Analysis of the data showed almost no correlation between grain

roundness and settling velocity, the main factors being sphericity and the Reynolds number. The data yield the modified Stokes equation for the prediction of the settling velocity, w_s ,

$$w_s = \frac{1}{18}\frac{1}{\mu}(\rho_s - \rho)gD_n^2\,(0.672 + 0.318E)$$

where ρ_s and ρ are respectively the particle and fluid densities, D_n is the grain nominal diameter, μ the fluid viscosity, and E is the grain shape factor (sphericity).

In the second experiments, settling velocities of natural quartz sand grains were measured in the settling tube containing water. Sand samples were sieved into 10 quarter-phi size ranges (-0.75 to 1.50ϕ). Each grain was measured under a microscope for its longest axial diameter, D_l , intermediate diameter, D_i , and grain roundness. It was found that the average D_i values are slightly smaller than the diagonal openings of the sieve screens. During the settling experiments, most of the grains showed very irregular motions such as oscillations and spinning. The larger the grain size, the larger these irregular motions. Analyses of the data showed almost no effect of roundness on the settling velocities. The intermediate diameters of the grains, D_i , showed the most consistent relationship to their settling velocities. An analysis procedure was arrived at wherein either D_i or the sieve diameter can be used in the equation of Gibbs, et al. (1971) to evaluate the settling rate of an "equivalent sphere", and then that value corrected to yield the average settling velocity of the natural sand grains.

EXPERIMENTS ON THE SETTLING BEHAVIOR OF IRREGULAR GRAINS IN A FLUID

by

Jumpei Baba

A THESIS

submitted to

Oregon State University

in partial fulfillment of

the requirements for the degree of

Masters of Science

Completed 20 May 1980

Commencement June 1981

APPROVED

Redacted for privacy

Professor of Oceanography in charge of major

Redacted for privacy

Dean of School of Oceanography

Redacted for privacy

Dean of Graduate School

Date thesis presented 2 July 1980

ACKNOWLEDGEMENTS

I would like to thank Dr. Paul D. Komar for his help and encouragement. I also thank Drs. Arthur Boucot, Kenneth Scheidegger and Robert Holman, who were members of my thesis committee, and Curt Peterson and Alan Morse for helping in the experiments.

TABLE OF CONTENTS

LIST OF FIGURES

LIST OF TABLES

PART I

SETTLING VELOCITIES OF IRREGULAR GRAINS AT LOW REYNOLDS NUMBERS

SETTLING VELOCITIES OF IRREGULAR GRAINS AT LOW REYNOLDS NUMBERS[1]

JUMPEI BABA and PAUL D. KOMAR

School of Oceanography
Oregon State University
Corvallis, Oregon 97331

ABSTRACT: Settling rates of irregular glass particles were measured in a settling tube containing glycerine, yielding Reynolds numbers equivalent to silt to very fine sand quartz grains settling in water. The glass particles were collected from beaches and so show varying degrees of rounding due to sand-blasting in the surf. Each was measured for its weight, roundness and grain shape (sphericity). Roundness was determined using Power's scale, having values from 0 to 6, corresponding to very angular particles to well rounded particles. Grain shape was defined in terms of the E shape factor of Janke. The ranges of particle weights, roundnesses and E shape factors are respectively 0.16-5.18 grams, 0.5-5.4 and 0.239-0.809.

The settling grains showed some irregular behavior such as oscillations, but generally maintained their maximum projection areas oriented perpendicular to the fall direction. Analysis of the data demonstrates almost no correlation between the settling velocity and the grain roundness, the main controlling factors being the grain shape and Reynolds number. Analysis of the data shows that the settling velocity w_s can be calculated with the modified Stokes equation

$$w_s = \frac{1}{18}\frac{1}{\mu}(\rho_s - \rho)\, g D_n^2\, (0.672 + 0.318E)$$

[1]Manuscript received ; revised

for particles having Reynolds numbers less than 0.5, where ρ_s and ρ are respectively the particle and fluid densities, D_n is the grain nominal diameter, μ the fluid viscosity, and E is the grain shape factor. A more complex relationship is presented that is applicable at higher Reynolds numbers.

INTRODUCTION

Natural sedimentary particles are irregular in overall shape as well as having a smaller-scale surface roughness (pits, groves, etc.). Such irregularities can of course affect the rate at which they settle in a fluid such as water. Yet nearly all previous studies have employed fairly regular if non-spherical grains: ellipsoids (Komar and Reimers, 1978), cylinders (McNown and Malaika, 1950; Komar, 1980), and even octahedrons and tetrahedrons (Pettyjohn and Christiansen, 1948). There have been few studies that employed irregular grains, probably due to the difficulty of quantifying the irregularities in a manner meaningful to grain settling. Albertson (1953) reported on measurements that included crushed gravel as well as naturally rounded gravel and noted that the angularity of the crushed gravel resulted in larger drag coefficients (reduced settling velocities). The measurements of Briggs, et al. (1962) using crushed heavy minerals included both shape and grain irregularity effects, but the two were not distinguished in the analysis. Only the study of Williams (1966) can be said to have approached the effects of particle roundness and surface texture in a systematic manner. But even in his study artificial (plastic) cylinders, disks and

spheres were employed with their edges having varying degrees of rounding and their surfaces uniformly pitted or groved.

The purpose of this study is to investigate the settling behavior of irregular particles that include the effects of non-sphericity, grain roundness, and grain asymmetries. A set of settling experiments has been undertaken for this purpose.

EXPERIMENTS

The experiments involved the settling of glass particles in glycerine. As in the experiments of Komar and Reimers (1978) with basalt pebbles settling in glycerine, the Reynolds numbers of the settling glass particles make the experiments hydraulically equivalent to the settling of silt to very-fine quartz sand in water. Thus the results will be applicable to sedimentary materials. The advantage of using the large glass particles rather than quartz silt grains directly is that the glass grains are large enough to make their weights directly measureable as well as increasing the accuracy of their size measurements.

The glass particles used in the experiments are "beach glass", fragments of broken bottles obtained from Oregon beaches. These have been, to varying degrees, rounded by the natural sand-blasting in the surf. Sharp edges tend to be rounded, and the surfaces may be frosted. Particles employed represent a wide range from sharply angular fresh glass to well rounded frosted grains. The grain roundness was quantified using the grain images provided by Powers (1953). The ρ_r logarithmic scale of Folk (1955) was employed which ranges from 0 (very angular) to 6 (well rounded) [see Blatt, et al. (1972, Fig. 3-18)]. Roundness

values for the 72 particles used in the study are given in Table 1, and are seen to range 0.5 to 5.4.

The weights and dimensions of the 72 grains are also given in Table 1. The three axial sizes of each particle were measured with a micrometer, D_l the longest axis and D_i and D_s the intermediate and shortest axes. In most cases the particles are roughly ellipsoidal in shape and so these three axial diameters are approximately mutually perpendicular. These axial diameters were used only to define the particle shape, not to define the nominal diameter of the particle, D_n, which was used as the length scale in the analysis of the grain settling. The nominal diameter was instead calculated from the more accurately measured particle weight, the nominal diameter being defined as the diameter of a sphere having the same weight and volume.

Several measures of grain shape have been proposed. Komar and Reimers (1978) demonstrated that in application to the settling of ellipsoidal grains the Corey shape factor is preferable to the Wadell sphericity definition. Komar (1980) in turn showed that if cylinders as well as ellipsoidal particles are included, the E shape factor introduced by Janke (1966) is preferred over the Corey shape factor. As defined by Janke, the E shape factor is given by

$$E = D_s \left[\frac{D_s^2 + D_i^2 + D_l^2}{3} \right]^{-1/2} \qquad (1)$$

For a sphere, E = 1.0; for non-spherical grains, $0 < E < 1.0$. Although the E shape factor is more complicated than the Corey shape factor and lacks any fluid mechanics basis, it will be employed in the analyses

TABLE 1.– *Glass particles settling data*

ID #	D_l (cm)	D_i (cm)	D_s (cm)	WEIGHT (gm)	ESF	ρ_r	w_s (cm/sec)	REYNS. NO.
1	2.331	1.132	1.044	4.329	0.6471	4.8	10.58	1.921
2	2.360	1.132	0.663	2.559	0.4255	4.4	7.02	1.071
3	1.498	1.086	0.626	1.660	0.5550	4.5	6.28	0.829
4	2.311	1.120	0.689	2.569	0.4487	4.7	7.99	1.220
5	1.729	1.099	0.804	2.001	0.6327	4.5	6.92	0.974
6	2.008	0.776	0.329	0.783	0.2618	2.2	3.36	0.345
7	1.676	1.248	0.483	1.759	0.3899	4.7	5.99	0.806
8	1.979	1.404	1.083	3.310	0.7057	3.1	9.45	1.569
9	1.645	1.040	0.592	1.686	0.5037	4.8	6.02	0.799
10	1.479	1.045	0.459	1.230	0.4256	4.9	5.00	0.597
11	1.715	0.950	0.529	1.096	0.4512	4.1	4.49	0.516
12	2.453	1.945	0.721	5.182	0.3888	4.6	10.46	2.018
13	2.300	1.337	0.590	3.754	0.3402	4.7	8.62	1.493
14	1.961	1.630	0.356	1.873	0.2394	5.1	5.34	0.734
15	2.288	1.598	0.557	2.788	0.3387	4.2	8.14	1.277
16	2.018	1.599	0.557	2.661	0.3662	5.5	7.33	1.132
17	1.645	1.111	0.444	1.181	0.3777	4.2	5.04	0.593
18	1.919	1.221	0.320	1.405	0.2413	3.8	4.47	0.558
19	1.566	1.146	0.537	1.441	0.4622	4.3	5.44	0.685
20	1.243	0.912	0.555	0.844	0.5882	4.2	4.23	0.446
21	1.957	1.140	0.431	1.258	0.3235	4.0	4.54	0.547
22	1.082	0.701	0.244	0.167	0.3222	0.5	1.32	0.081
23	1.069	0.383	0.334	0.160	0.4888	1.8	1.30	0.079
24	1.701	1.015	0.508	1.246	0.4305	5.0	5.13	0.615
25	1.061	0.585	0.327	0.211	0.4515	2.7	1.55	0.103
26	1.080	0.858	0.460	0.642	0.5481	4.8	3.63	0.349
27	1.072	0.920	0.460	0.714	0.5360	5.1	3.73	0.371
28	1.427	0.736	0.562	0.816	0.5719	4.8	4.00	0.417
29	1.404	0.851	0.579	0.965	0.5757	4.8	4.71	0.519
30	0.685	0.586	0.311	0.176	0.5651	4.1	1.44	0.090
31	1.836	1.408	0.564	2.1949	0.4100	3.8	6.96	1.009
32	1.859	1.071	0.486	1.402	0.3826	4.0	5.30	0.662
33	1.867	0.968	0.513	1.241	0.4108	4.1	4.83	0.579
34	1.609	0.631	0.496	0.831	0.4781	4.4	3.89	0.408
35	1.938	0.947	0.518	1.359	0.4046	5.4	4.91	0.606
36	1.369	0.897	0.448	0.809	0.4570	4.2	3.81	0.396

TABLE 1.– *Continued*

ID #	D_l (cm)	D_i (cm)	D_s (cm)	WEIGHT (gm)	ESF	ρ_r	w_s (cm/sec)	REYNS. NO.
37	1.070	0.776	0.641	0.706	0.7558	4.1	3.90	0.388
38	1.632	0.869	0.367	0.861	0.3368	4.2	4.04	0.429
39	1.753	0.830	0.388	0.886	0.3395	5.1	4.04	0.432
40	1.407	1.101	0.380	0.983	0.3589	4.2	4.06	0.451
41	1.355	0.666	0.479	0.569	0.5239	3.9	3.18	0.294
42	1.250	0.522	0.409	0.358	0.5002	3.6	2.51	0.199
43	1.126	0.885	0.381	0.458	0.4451	4.7	2.92	0.251
44	1.401	1.209	0.557	1.364	0.4988	4.1	5.48	0.678
45	1.458	1.165	0.532	1.026	0.4751	4.2	5.00	0.562
46	1.272	0.754	0.380	0.562	0.4310	4.1	3.32	0.306
47	1.071	0.821	0.354	0.411	0.4391	3.9	2.80	0.232
48	1.501	1.138	0.376	0.963	0.3389	4.0	4.18	0.460
49	1.093	0.669	0.249	0.271	0.3308	4.3	1.99	0.144
50	1.475	0.961	0.371	0.781	0.3572	4.3	3.76	0.386
51	1.145	0.848	0.353	0.573	0.4168	3.1	3.31	0.307
52	1.487	1.192	0.371	0.959	0.3416	3.7	4.14	0.456
53	1.275	0.454	0.355	0.229	0.4398	3.4	1.39	0.095
54	0.947	0.637	0.497	0.283	0.6910	4.2	2.06	0.151
55	0.801	0.582	0.253	0.161	0.4278	3.0	1.18	0.072
56	0.800	0.462	0.308	0.145	0.5486	3.2	1.24	0.072
57	1.051	0.599	0.413	0.339	0.5589	4.4	2.04	0.159
58	0.700	0.677	0.305	0.239	0.5174	4.0	1.71	0.118
59	0.689	0.520	0.456	0.202	0.8093	4.4	1.71	0.112
60	1.118	0.466	0.315	0.251	0.4358	4.1	1.87	0.132
61	0.731	0.510	0.420	0.198	0.7388	3.2	1.58	0.103
62	0.916	0.569	0.325	0.166	0.4995	3.7	1.44	0.088
63	0.881	0.651	0.376	0.288	0.5619	4.1	1.85	0.136
64	0.739	0.466	0.188	0.121	0.3643	4.1	1.01	0.056
65	1.044	0.718	0.252	0.249	0.3371	3.9	1.65	0.116
66	0.948	0.650	0.298	0.234	0.4352	4.3	1.55	0.106
67	0.920	0.507	0.315	0.194	0.4970	3.7	1.52	0.098
68	0.683	0.568	0.444	0.222	0.7744	3.8	1.90	0.128
69	0.709	0.497	0.321	0.125	0.6027	4.3	1.14	0.063
70	0.828	0.351	0.280	0.110	0.5146	3.6	1.08	0.058
71	0.917	0.480	0.178	0.079	0.2443	4.1	0.79	0.038
72	0.795	0.409	0.327	0.119	0.5945	2.8	1.18	0.065

to follow since it has been demonstrated to be applicable to a wide range of grain shapes (Janke, 1966; Komar, 1980). Table 1 lists the values of E for the 72 glass particles, calculated from the D_s , D_i and D_l measurements using equation (1); the complete range is 0.239-0.809.

Roundness and sphericity are conceptually different measurements of grain shape (Wadell, 1932). This is demonstrated in Figure 1 for the glass particles, plotting the measured roundness (ρ_r) values versus the E shape factors. This lack of correlation between the two is also important in the analyses to follow.

No attempts have been made to quantify the grain surface texture, that is, the degree to which the particle surfaces are pitted or grooved. Williams (1966) demonstrated that grain roundness and shape (sphericity) are much more important than surface roughness, and this is also to be expected from a fluid mechanics analysis of drag. Of importance to the grain settling behavior are the asymmetries of the particles. Such asymmetries will be the main cause of an unbalance of forces acting on the particles that sets them to oscillating or tumbling. Only a very detailed analysis of each grain might resolve the balance of forces acting on the asymmetric grain as it settles and continuously reorients itself. Such an analysis is beyond the scope of the present study. These effects can be expected to be greater at higher Reynolds numbers than included in the present experiments. This will be discussed later in the paper following the data analysis.

Grain densities are required in the analyses, but the grain irregularities precluded their direct determinations. The colors of the particles were various shades to browns, greens, and transparent, indicating

Figure 1: Grain shape as defined by E of equation (1) versus the grain roundness ρ_r for the 72 glass particles used in the experiments.

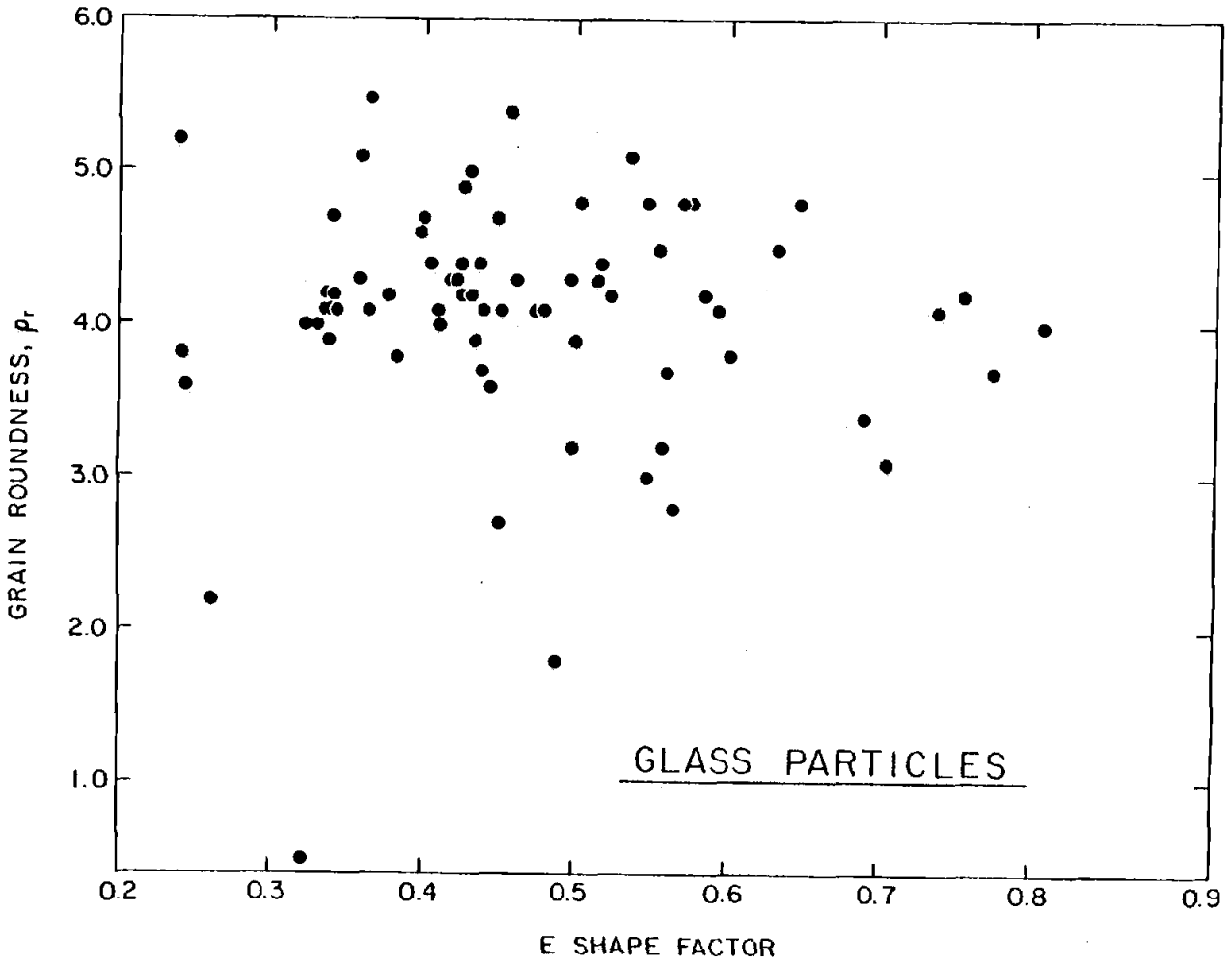
6.0
5.0
4.0
3.0
2.0
1.0
GRAIN ROUNDNESS, ρ_r
0.2
0.3
0.4
0.5
0.6
0.7
0.8
0.9
E SHAPE FACTOR
GLASS PARTICLES

a source from broken beer, wine and pop bottles (in spite of Oregon's bottle bill). The densities of several popular beverage bottles were determined by weighing them and obtaining their volumes by immersion in water contained in a graduated cylinder. The average density was found to be 2.41 g/cm^3 (total range 2.39-2.44 g/cm^3). This average value is used throughout the analyses for the particle densities.

The experimental procedures for measuring the settling velocities were the same as those reported in Komar and Reimers (1978). The same 216-cm long, 33-cm inside diameter cylindrical settling tube was employed, again filled with glycerine. All particles were found to settle with their maximum projection areas (defined by D_l and D_i) perpendicular to the settling direction. In order to insure that the particles quickly achieved their steady terminal velocities, they were released with this orientation. Although on average they maintained this orientation while settling, due to their shape irregularities the particles usually had secondary motions superimposed on the direct settling. This usually involved a slight oscillation to-and-fro at right angles to the settling direction. Such excursions from direct settling were in all cases small. The particles were not observed to tumble or spin.

The resulting measured settling velocities are given in Table 1. Also given are the Reynolds numbers of the form $Re = \rho w_s D_n/\mu$, ρ and μ being the fluid density and absolute viscosity. The Reynolds number range is 0.04 to 2.02 so that much of the data is in the Stokes range ($Re < 0.5$). As already indicated, these Reynolds numbers approximately correspond to quartz grains in the silt to very fine sand sizes settling in water.

DATA ANALYSIS

Preliminary multiple regression analysis of the data indicated that the grain shape, E, is much more important than the grain roundness, ρ_r, in determining the grain settling velocity. For this reason, the analysis procedure has been to first concentrate on the effects of shape, remove those effects, and then to assess any residual influence due to the grain roundness or the value of the Reynolds number.

Based on the ellipsoidal-pebble data of Komar and Reimers (1978) and additional data on the settling of cylinders, Komar (1980) determined empirically that

$$w_s = \frac{1}{18}\frac{1}{\mu}(\rho_s - \rho)\, g\, D_n^2\, E^{0.380} \qquad (2)$$

for Reynolds numbers $Re < 0.5$ (Stokes range). For a sphere $E = 1.0$ and D_n becomes the grain diameter, so that equation (2) reduces to the well-known Stokes equation

$$w_s\text{-Stokes} = \frac{1}{18}\frac{1}{\mu}(\rho_s - \rho)\, g\, D_n^2 \qquad (3)$$

The presence of the E shape factor in equation (2) broadens its application to ellipsoidal and cylindrical shapes as well as spheres.

The present data on the settling of glass particles could be compared directly to equation (2). Instead of this direct approach, Figure 2 compares the measured w_s value, divided by w_s-Stokes of equation (3), to the grain E shape factor. The curve of equation (2) is shown for comparison. It is apparent that the new data follow

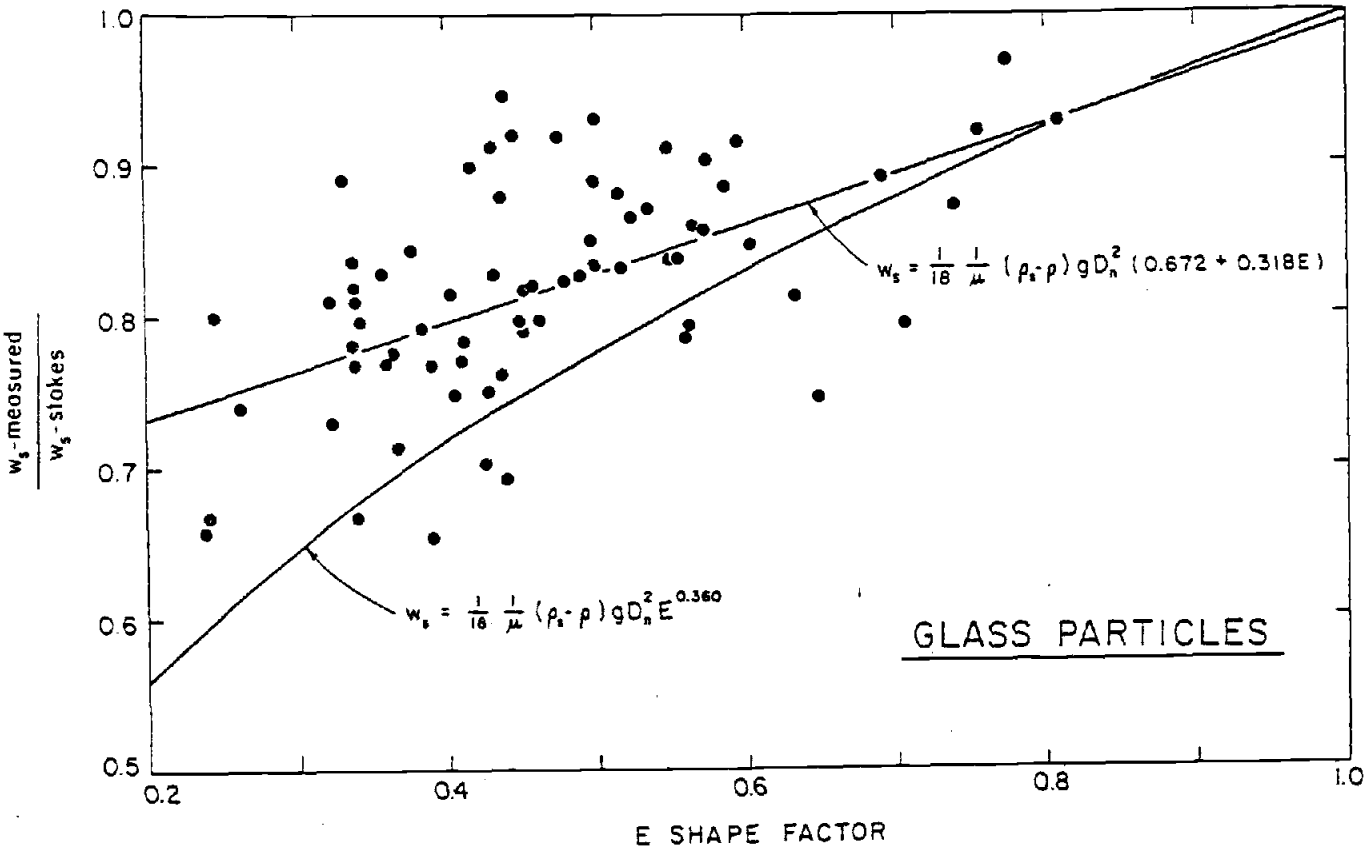

Figure 2: Comparison of the settling velocity to the E shape factor. The straight-line fit to the data yields equation (4). The curve is that obtained by Komar (1980) for regularly-shaped particles.

the trend of equation (2) but also show a systematic departure. Such a departure from equation (2) is not surprising in that it was based on completely regular, symmetric grains. What is surprising in Figure 2 is that the measured settling velocities of the irregular grains are greater than predicted by equation (2). It was anticipated that the grain irregularities would reduce the grain settling velocities, both because of the induced oscillations in the settling and because of the increased surface area per unit grain weight, tending to increase the surface drag. The only way we can think to explain the increased settling rate is in the reduction of the true projection area. For a completely regular ellipsoidal grain the projection area is the full ellipse defined by the D_l and D_i axes. For the irregular grains, the actual projection area is somewhat less than this ellipse, the amount of the departure probably increasing with decreasing E. It should be pointed out that the grains are settling more slowly than spherical grains of the same weight, but this reduction in settling velocity is due to the overall non-sphericity of the grains, not because of their irregularities. The conclusion is that the regular, symmetric non-spherical grains have greater reductions in settling velocities from spheres than do the irregular, non-spherical grains. It is possible and probable that this conclusion applies only to the low Reynolds numbers of the experiments in this study (the Stokes region). At higher Reynolds numbers the grains are more apt to spin, tumble and have larger oscillations, and these irregularities may be expected to cause a decrease in their settling velocities.

Linear regression of the data of Figure 2 yields the straight line shown, having the equation

$$w_s = \frac{1}{18}\frac{1}{\mu}(\rho_s - \rho)\, g\, D_n^2\, (0.672 + 0.318E) \qquad (4)$$

It is seen that equation (4) nearly becomes the Stokes relationship, equation (3), when E = 1.0 (spheres); this is also seen in Figure 2 where w_s-measured/w_s-Stokes $\simeq$ 1.0 when E = 1.0. Figure 3 compares the measured settling velocity with w_s predicted by equation (4). It is seen that there is a progressive departure at higher values of w_s and that this departure results from the Reynolds number being beyond the range of Stokes settling. Thus equation (4) should be limited in application to $Re < 0.5$. In that range $R^2 = 0.986$.

Equation (4) can be used to account for much of the shape effects on the grain settling, allowing an improved chance of detecting any influence the grain roundness might have. Figure 4 plots the w_s-measured divided by the w_s-predicted of equation (4) versus the measured grain roundness, ρ_r. There is a lack of any significant correlation, reconfirming the results of the multiple regression analysis.

A similar plot is presented in Figure 5 for an analysis of the Reynolds number dependence. This figure further demonstrates the departure from equation (4) as the Reynolds number increases above Re = 0.5 and the Stokes range. For $Re > 0.5$ the straight-line fit to the data yields

$$w_s = \frac{1}{18}\frac{1}{\mu}(\rho_s - \rho) g D_n^2\, (0.672 + 0.318E)(1.057 - 0.111Re) \qquad (5)$$

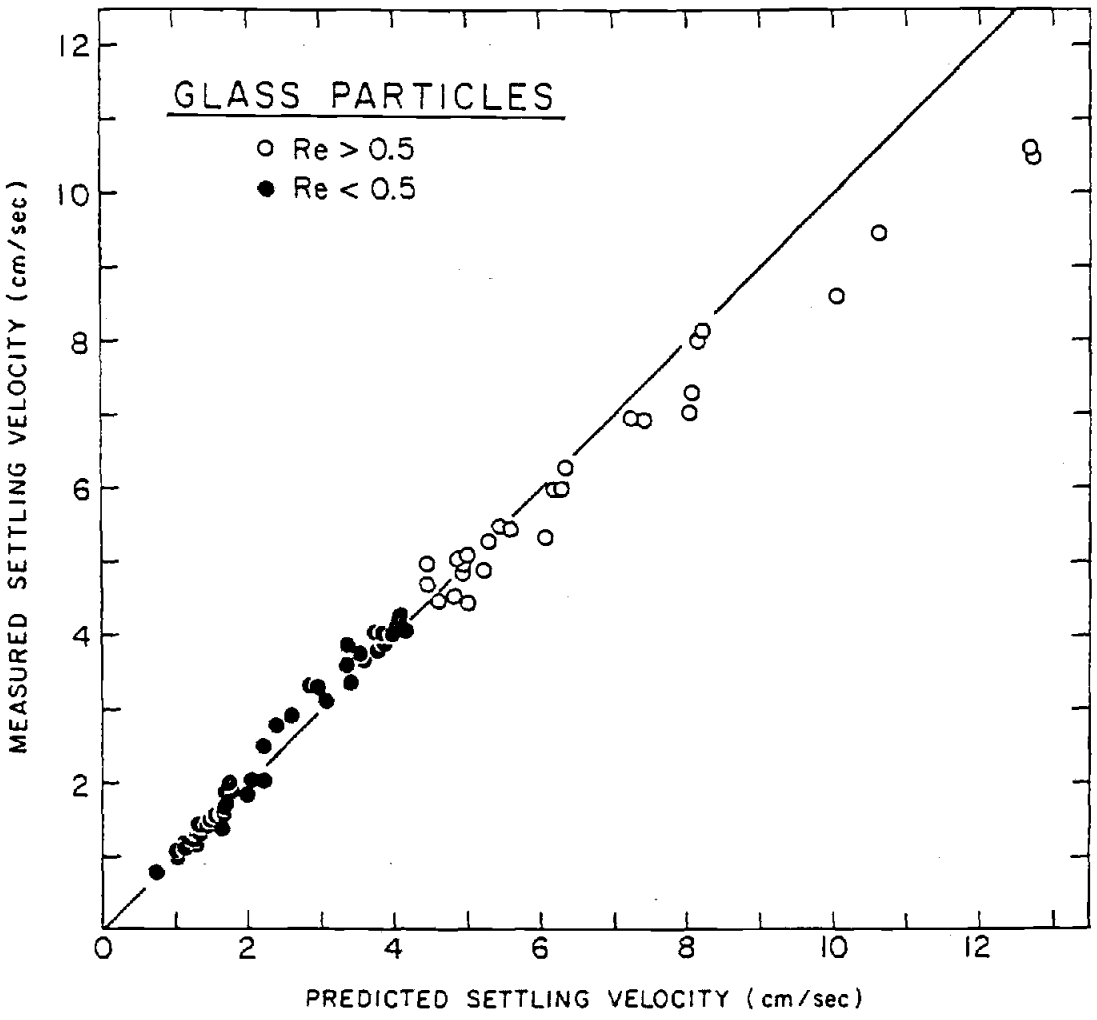

Figure 3: The measured settling velocity w_s prediction by equation (4). The data in the Stokes region (Re < 0.5) show good agreement (R^2 = 0.986) but the data for Re > 0.5 show a progressive departure.

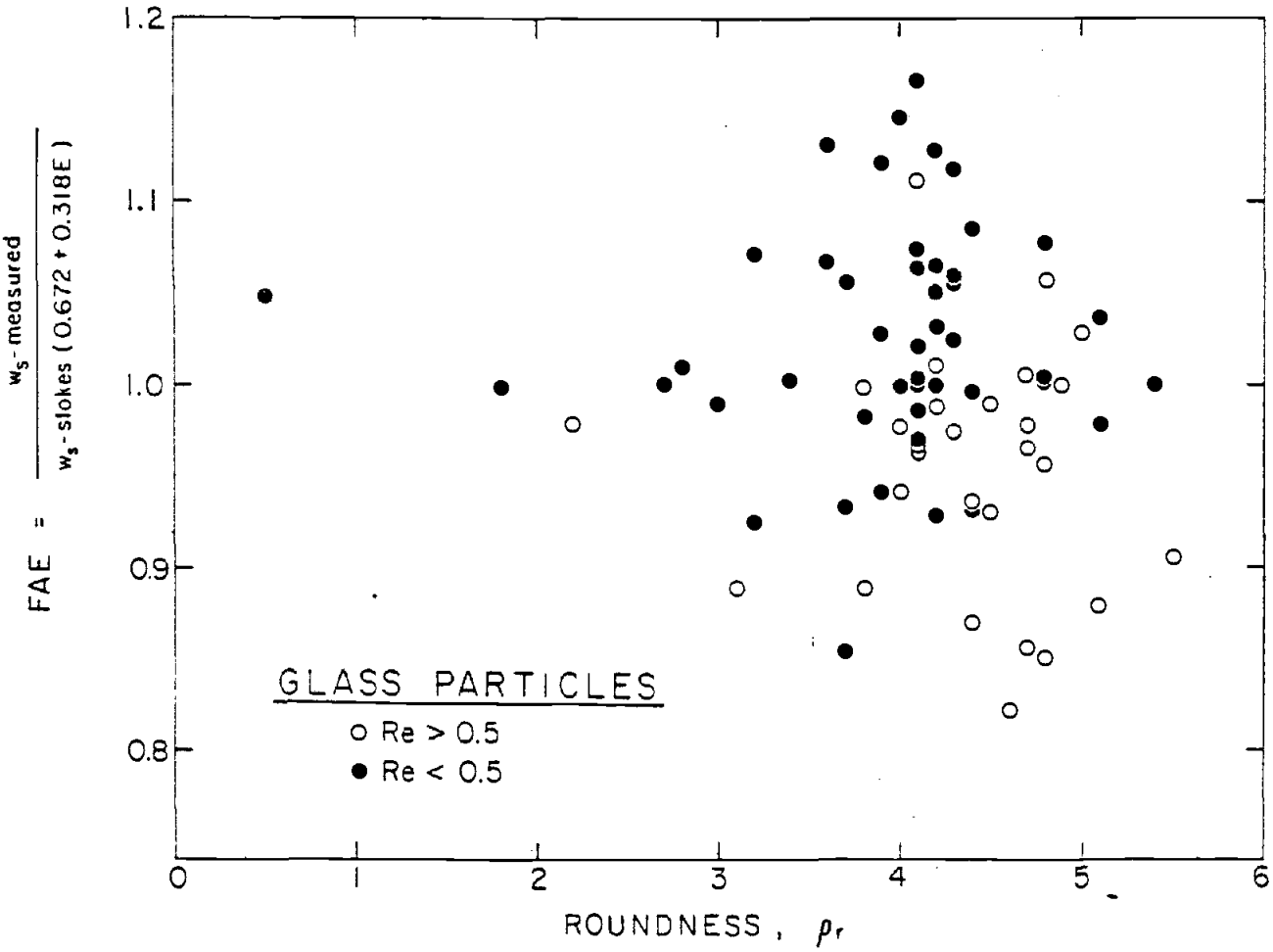

Figure 4: The measured settling velocities, normalized to remove the effects of grain shape, compared to the measured grain roundness, demonstrating the lack of any dependence.

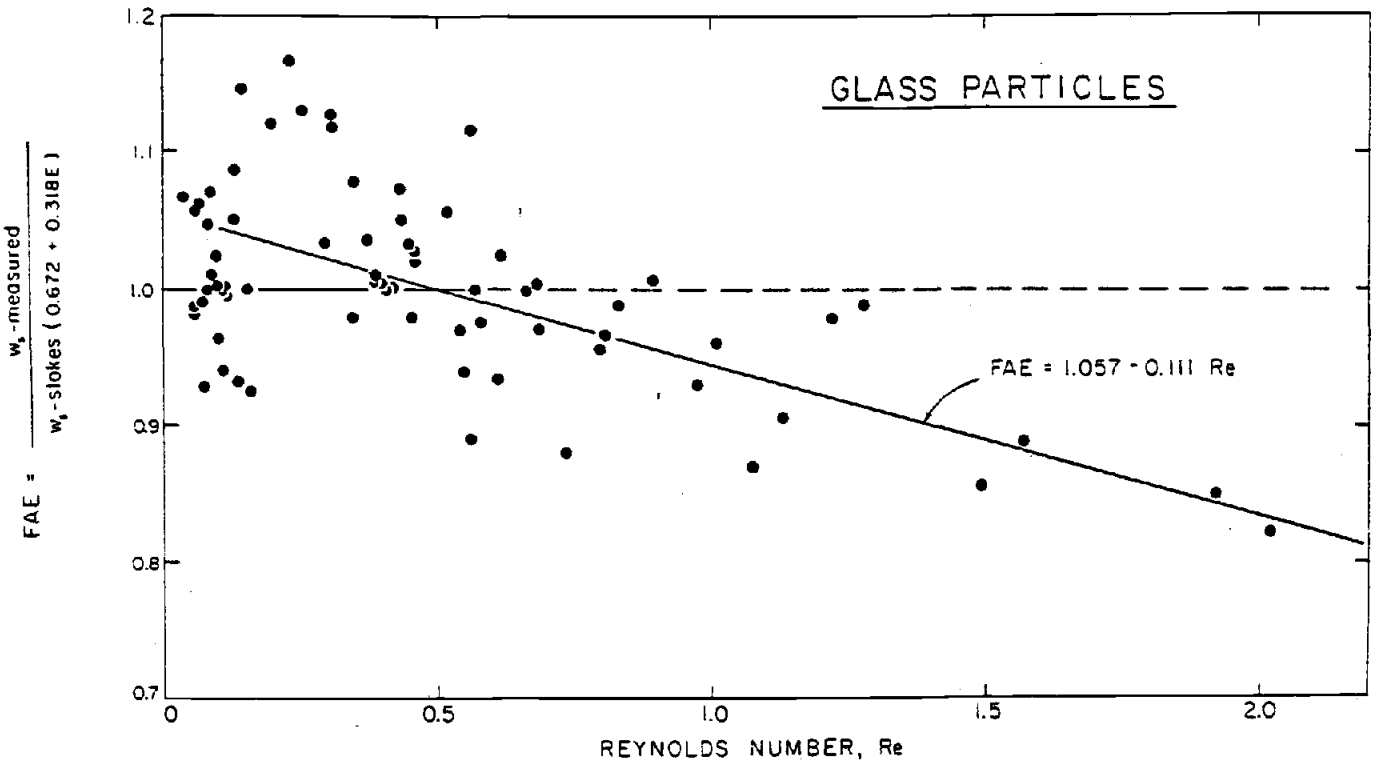

Figure 5: Dependence of the settling velocity on the Reynolds number, showing an approximate linear departure from equation (4) for Re > 0.5. The straight-line fit shown yields equations (5) and (6).

This form of the equation is inconvenient to use since $Re = \rho w_s D_n/\mu$ contains the settling velocity w_s. However, equation (5) can be solved for w_s, yielding

$$w_s = \frac{1.057 w_e}{1.0 + 0.111 \rho D_n w_e/\mu} \qquad (6)$$

where w_e is the settling velocity as calculated with equation (4), taking into account the grain shape as defined by E. In Figure 6 the measured w_s values are plotted against w_s predicted with equation (6). There is seen to be a very good correlation ($R^2 = 0.99$). A comparison with Figure 4 shows that equation (6) is applicable to higher Reynolds numbers than equation (4), at least up to $Re \simeq 2.0$, the limit of our data. The simpler equation (4) can be used rather than equation (6) when $Re < 0.5$ (Stokes region).

SUMMARY OF CONCLUSIONS

1. The effects of grain roundness on the settling velocity are much smaller than shape effects (non-sphericity), being undetectable in the present experiments.
2. Irregular grains settle faster than regular, symmetrical grains of the same weight and having the same general shape as defined by the E shape factor. This is probably due to the smaller projection areas of the irregular grains perpendicular to the fall direction.
3. The above conclusions may be true only for low Reynolds numbers

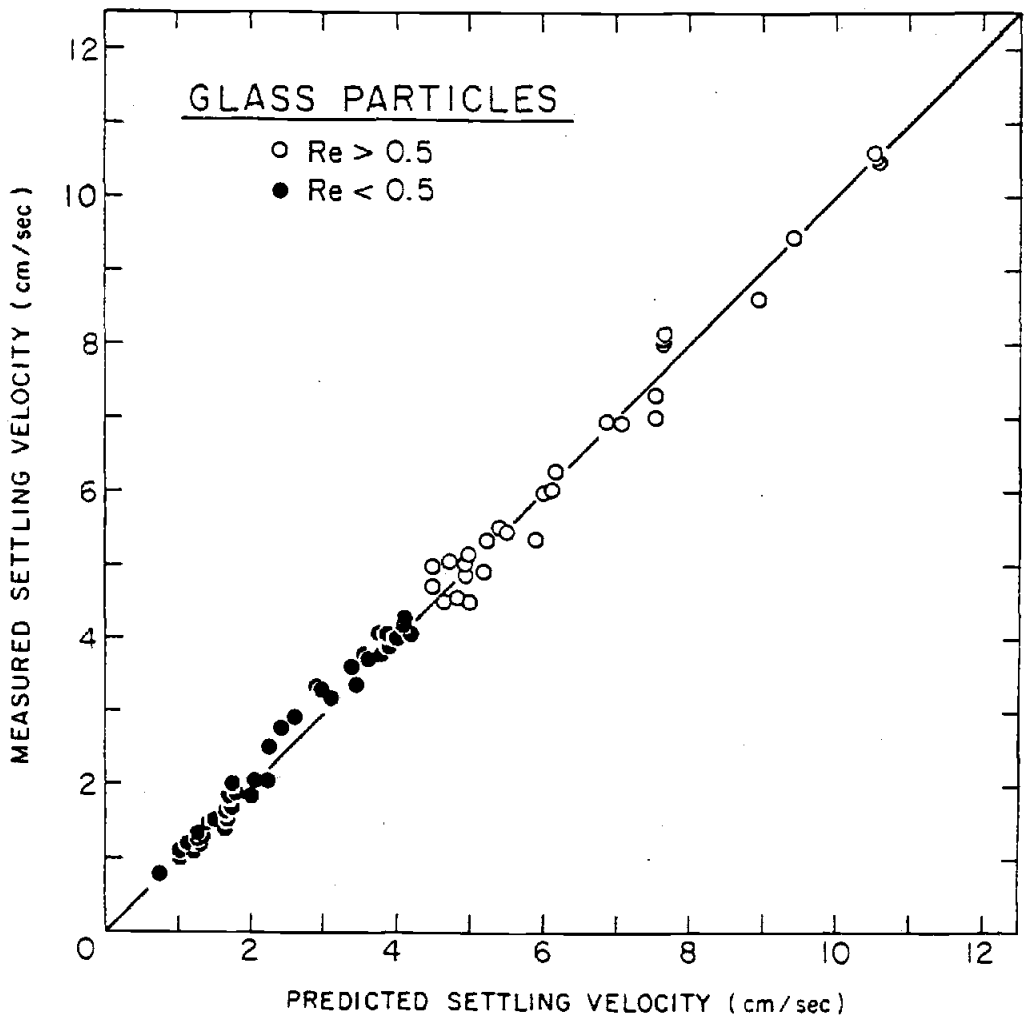

Figure 6: The measured settling velocity versus w_s predicted by equation (6). A comparison with Fig. 3 shows that equations (4) and (6) are equally good for Re < 0.5, but equation (6) gives much better results for Re > 0.5. The over-all fit is $R^2 = 0.99$.

(Re < 2.0). At higher Reynolds numbers where grains tend to spin, tumble or have larger oscillations, the conclusions may be different.

4. Equation (4) can be used to predict the settling velocities of irregular grains for Re < 0.5 (Stokes settling). The more complex equation (6) extends the application to Re < 2.0.

ACKNOWLEDGEMENTS

We would like to thank Curt Peterson for his help in conducting the grain settling experiments.

REFERENCES

ALBERTSON, M.L., 1953, Effect of shape on the fall velocity of gravel particles: Proc. 5th Iowa Hydraulics Conf., Iowa City, p. 243-261.

BLATT, H., MIDDLETON, G., and MURRAY, R., 1972, Origin of Sedimentary Rocks: Prentice-Hall, Inc., Englewood Cliffs, N.J., 634 p.

BRIGGS, L.I, McCULLOCH, D.S., and MOSER, F., 1962, The hydraulic shape of sand particles: Jour. of Sedimentary Petrology, v. 32, p. 645-656.

FOLK, R.L., 1955, Student error in determination of roundness, sphericity and grain size: Jour. Sed. Petrology, v. 25, p. 297-301.

JANKE, N.C., 1966, Effect of shape upon the settling velocity of regular convex geometric particles: Jour. Sed. Petrology, v. 36, p. 370-376.

KOMAR, P.D., 1980, Settling velocities of circular cylinders at low Reynolds numbers: Jour. of Geology, v. 88, p. 327-336.

KOMAR, P.D, and REIMERS, C.E., 1978, Grain shape effects on settling rates: Jour. of Geology, v. 86, p. 193-209.

McNOWN, J.S., and MALAIKA, J., 1950, Effects of particle shape on settling velocity at low Reynolds numbers: Trans. Amer. Geophys. Union, v. 31, p. 74-82.

PETTYJOHN, E.S., and CHRISTIANSEN, E.B., 1948, Effect of particle shape on free-settling rates of isometric particles: Chemical Engineering Progress, v. 44, n. 2, p. 157-172.

POWERS, M.C., 1953, A new roundness scale for sedimentary particles: Jour. Sed. Petrology, v. 23, p. 117-119.

WILLIAMS, G.P., 1966, Particle roundness and surface texture effects on fall velocity: Jour. Sed. Petrology, v. 36, p. 255-259.

PART II

MEASUREMENTS AND ANALYSIS OF SETTLING VELOCITIES OF NATURAL QUARTZ SAND GRAINS

MEASUREMENTS AND ANALYSIS OF SETTLING VELOCITIES OF NATURAL QUARTZ SAND GRAINS[1]

JUMPEI BABA and PAUL D. KOMAR

School of Oceanography
Oregon State University
Corvallis, Oregon 97331

ABSTRACT: Settling velocities in water were measured for natural quartz sand grains in the size range -0.75 to 1.50ϕ (0.35-1.68 mm). Obtained from beach sands, the grains were selected so as to provide a wide range of roundness from very angular to very well rounded (ρ_r = 0.6 - 5.1). For each grain two axial diameters were measured under a microscope, the longest axial diameter, D_l , and the intermediate diameter, D_i . Settling velocities were measured in a 6-meter long settling tube.

The axial diameters D_i and D_l are compared with the dimensions of the screen openings of the sieves, and it is found that on average D_i is slightly less than the diagonal of the screen opening. The measured settling velocity, w_m , is then compared with the settling velocity of a sphere, w_s , calculated using D_i as the sphere diameter, and the relationship $w_m = 0.761w_s$ is found to be consistent with the data. The analysis shows that the grain roundness has no measureable effect on the settling rate. It is believed that the measured settling velocities are less than those of spheres because the natural grains are nonspherical and asymmetric, factors which cause them to oscillate and spin as they settle.

---

[1]Manuscript received ; revised

The results provide graphs and empirical equations which permit the evaluation of actual grain settling rates (rather than settling velocities of spheres) from sieve sizes or from microscopic measurements of D_i for individual grains.

INTRODUCTION

A knowledge of the settling rates of natural sand grains is basic to sediment transport considerations and to the determinations of grain size distributions through grain settling. In most applications we are satisfied to assume that the grains are spherical in order to utilize the well-established equations or curves based on the perfect sphere. Natural sand grains are of course highly irregular in shape and in the degree of roundness, factors which will affect their settling behaviors and rates.

Considering the fundamental importance of sand grain settling, it is surprising how few measurements have been made to assess the effects of natural grain irregularities. Lane (1938) presents a graph of the settling rates of quartz sedimentary particles versus grain diameter. The data were obtained by the U.S. Bureau of Reclamation, but no details are given as to the measurement techniques. Below a grain diameter of about 0.5mm the data show good agreement with the expected settling rates of perfect spheres. Above that size there is a marked departure with the natural sand grains settling at significantly slower rates than the spheres.

Mamak (1964) presents a table of average settling rate versus grain diameter, but without giving the actual data upon which the table is based. His results also show that the settling rates of natural grains smaller than 0.1mm are in good agreement with the settling rates of spheres, but for

larger grains there is a considerable reduction of the settling rates of the sedimentary grains versus the spheres. In their general review of settling-velocity curves, Graf and Acaroglu (1966) mentioned that their data are in good agreement with that of Mamak (1964), but without actually presenting any data.

These former studies have established that above a grain size of about 0.1-0.5 mm, the settling velocities of natural sand grains depart markedly from the settling rates of spheres. The purpose of this present study is to obtain additional data on the settling behavior and rates of natural sedimentary grains, and to examine the importance of grain irregularities in producing the observed reduction in settling velocities from those of spheres.

EXPERIMENTS

The particles employed in this study are natural quartz sand grains collected from Oregon beaches. A composite sample was accumulated to provide a wide range of grain sizes. This sample was carefully sieved using standard sieving techniques (Folk, 1964) into ten quarter-phi intervals ranging from -0.75 to 1.50ϕ (0.35-1.68 mm). Each sieve fraction contained various types of minerals. Only transparent quartz grains were selected so as to give a constant grain density in the analyses and because of the particular importance of quartz in most sediment transport considerations. From each sieve fraction a number of grains were selected so as to give a large range in degree of grain roundness. The roundness of each grain was determined using the images introduced by Powers (1953) together with the ρ_r logarithmic roundness scale of Folk (1955) [see

Blatt, et al. (1972, Fig. 3-18)]. The roundness values for the 229 grains selected are given in Table 1, and range from 0.6 (very angular) to 5.1 (very well rounded).

Particle sizes were then measured under the microscope. Since the particles are roughly ellipsoidal, they tend to rest in positions with their largest projection areas parallel to the glass slide. Therefore, two axial diameters can be readily measured for each grain by simple microscopic observations, the particle's longest axis, D_l , and intermediate axis, D_i . No attempt was made to measure the shortest axial diameter, that perpendicular to the glass slide. This unfortunately precludes the possibility of analyzing the data for grain sphericity effects, known to be important to grain settling (Komar, 1980 ; Baba and Komar, in press). Values of D_i and D_l for the 229 grains are given in Table 1.

The settling velocities were measured in a 6-meter long, plastic, cylindrical tube, 11.4 cm inside diameter, filled with fresh water. Times of descent were measured over a 5-meter length of the tube, the upper line being 65 cm from the top of the tube so as to insure that the grains reach terminal velocity before timing their rates. The long tube length was necessary to yield accurate measurements of the faster settling rates. The largest grains settle at rates up to 20.7 cm/sec (Table 1), which involves an elapsed time of 24.2 seconds over the 5-meter interval. The smallest grains took some 1.75 minutes. A Hewlett-Packard 55 pocket calculator with a digital timer was used in the experiments, permitting time measurements accurate to about 0.1 sec. Repeated settlings of a single grain were not attempted so we are unable to assess the repeatability of the measured rates. However, in their experiments on the settling of

TABLE 1.

ø size	NO.	D_l (mm)	D_i (mm)	ρ_r	W_m (cm/sec)	W_m / W_s	
- 0.75	1	1.94	1.50	4.8	20.64	0.943	
	2	3.10	1.40	4.2	18.73	0.907	
	3	2.50	1.70	3.4	19.00	0.785	
	4	2.40	2.00	3.1	20.65	0.751	
- 0.50	5	1.54	1.42	5.1	17.66	0.845	
	6	1.60	1.54	2.1	17.78	0.795	
	7	1.64	1.44	2.2	17.94	0.848	
	8	1.80	1.56	2.8	16.72	0.740	
	9	1.76	1.50	3.7	19.74	0.902	
	10	2.23	1.72	1.7	19.73	0.807	
	11	2.05	1.92	4.3			*
	12	2.38	2.12	1.5	15.64	0.544	
	13	2.30	2.23	3.2	17.58	0.589	
	14	2.00	1.95	3.1	18.10	0.671	
	15	2.30	1.77	2.2	15.31	0.612	
	16	2.12	1.72	4.1	19.10	0.782	
	17	2.25	2.00	2.7	17.54	0.638	
	18	2.53	2.00	3.3	19.28	0.701	
	19	2.61	1.61	2.2	18.34	0.791	
	20	1.61	1.54	3.9	19.94	0.892	
	21	2.70	1.95	3.2	18.07	0.670	
	22	1.79	1.74	3.3	17.94	0.727	
	23	1.66	1.51	2.9	19.30	0.877	
	24	1.94	1.64	2.7	19.16	0.814	
	25	2.28	1.59	4.0	19.14	0.834	
	26	2.51	1.87	2.7			*
	27	2.27	1.61	3.4	18.37	0.775	
	28	1.74	1.57	3.7	17.63	0.776	
	29	2.15	1.92	3.1	17.19	0.645	
- 0.25	30	1.74	1.64	4.3	14.93	0.635	
	31	2.28	2.07	0.7	11.65	0.413	
	32	1.69	1.48	3.2	17.79	0.794	
	33	1.72	1.38	2.7	15.77	0.772	
	34	2.00	1.72	2.6	17.01	0.696	
	35	1.95	1.59	3.4			*
	36	1.74	1.66	3.6			*
	37	1.89	1.79	1.8	15.38	0.610	
	38	2.10	1.59	2.8	17.58	0.766	
	39	1.59	1.46	3.3	17.60	0.822	
	40	1.84	1.80	3.8			*
	41	2.28	1.43	2.7	16.78	0.798	
	42	1.66	1.66	3.3	18.10	0.762	
	43	1.79	1.51	2.1	17.15	0.780	
	44	1.77	1.69	2.2	15.14	0.628	
	45	1.95	1.48	3.2			*

TABLE 1. - (Continued)

ϕ size	NO.	D_1 (mm)	D_i (mm)	ρ_r	W_m (cm/sec)	W_m / W_s	
- 0.25	46	2.20	1.72	2.2			*
	47	1.93	1.54	2.6			*
	48	1.95	1.43	4.2	16.30	0.775	
	49	1.93	1.41	3.2	15.36	0.739	
	50	2.10	1.38	2.8	17.48	0.856	
	51	1.79	1.74	3.1			*
	52	1.87	1.46	3.5	18.39	0.859	
	53	1.88	1.50	1.6	16.82	0.769	
	54	1.81	1.54	3.2	19.49	0.872	
± 0.00	55	1.56	1.28	3.2	16.46	0.8591	
	56	1.69	1.42	3.0			*
	57	1.79	1.44	3.1			*
	58	1.51	1.46	3.4			*
	59	1.84	1.56	3.2	16.39	0.725	
	60	1.92	1.15	3.6	15.16	0.868	
	61	1.66	1.43	4.1	15.36	0.730	
	62	2.28	1.05	1.7	14.35	0.891	
	63	1.92	1.46	3.0	14.57	0.681	
	64	1.41	1.23	2.7			*
	65	2.05	1.20	3.9	14.12	0.779	
	66	1.59	1.43	3.0	14.74	0.701	
	67	1.59	1.32	4.4	12.92	0.657	
	68	1.74	1.13	1.8	14.78	0.599	
	69	2.05	1.36	2.1	14.81	0.734	
	70	1.46	1.24	3.2	15.02	0.806	
	71	1.77	1.13	3.6			*
	72	1.46	1.16	2.2	14.48	0.823	
	73	1.84	1.43	3.0	16.14	0.763	
	74	1.84	1.46	2.1	16.21	0.758	
	75	1.66	1.15	4.6	15.55	0.891	
	76	1.51	1.23	2.6	16.40	0.886	
	77	1.66	1.28	2.5			*
	78	1.72	1.31	2.9	16.06	0.822	
	79	1.64	1.23	1.3	13.94	0.738	
+ 0.25	80	1.72	1.15	3.1	14.41	0.826	
	81	1.84	1.13	1.8	12.92	0.752	
	82	1.20	1.18	3.9	13.46	0.754	
	83	1.43	1.41	1.7	10.23	0.492	
	84	1.87	1.13	2.2	15.31	0.890	
	85	1.97	1.15	1.1	9.96	0.570	
	86	1.41	1.13	3.8	13.85	0.806	
	87	1.77	1.23	2.8	12.53	0.677	
	88	1.56	1.10	2.9	13.58	0.809	
	89	1.64	1.02	2.6	12.89	0.822	
	90	1.51	1.38	2.2	12.21	0.598	
	91	1.31	1.02	3.3	14.42	0.919	

TABLE 1. - (Continued)

ϕ size	NO.	D_l (mm)	D_i (mm)	ρ_r	W_m (cm/sec)	W_m / W_s	
+ 0.25	92	1.59	1.11	1.9	11.88	0.720	
	93	1.23	1.13	3.7	16.04	0.933	
	94	1.63	1.36	2.8			*
	95	1.41	1.15	2.3	13.27	0.760	
	96	1.25	1.05	3.2	14.96	0.929	
	97	1.56	1.23	2.9			*
	98	1.38	1.01	2.8			*
	99	1.41	1.32	1.0	12.48	0.635	
	100	1.51	1.05	3.6	14.81	0.920	
	101	1.36	1.08	3.2	12.74	0.772	
	102	1.33	1.05	3.0	13.38	0.831	
	103	1.36	1.20	2.8	14.52	0.802	
	104	1.36	0.97	4.2	14.87	0.993	
+ 0.50	105	1.43	1.00	1.8	12.01	0.780	
	106	1.10	0.97	2.0	11.32	0.756	
	107	1.20	1.02	1.8	9.68	0.618	
	108	1.08	1.00	3.1	11.13	0.723	
	109	1.23	0.96	1.6	10.27	0.692	
	110	1.31	0.92	3.4			*
	111	1.23	0.96	1.6	10.27	0.930	
	112	1.45	0.92	3.1	11.34	0.787	
	113	1.36	1.06	1.9	11.94	0.736	
	114	1.10	0.90	3.8	12.17	0.871	
	115	1.05	0.87	2.3	11.05	0.817	
	116	1.05	0.95	3.7			*
	117	1.41	1.25	2.7	11.72	0.625	
	118	1.15	0.92	3.1	10.98	0.762	
	119	1.20	0.85	2.2	10.62	0.802	
	120	1.25	1.01	3.8	11.32	0.729	
	121	1.22	1.01	2.3	12.85	0.827	
	122	1.02	0.90	3.8	13.29	0.951	
	123	1.23	1.00	2.8	12.06	0.783	
	124	1.16	1.08	1.7	12.35	0.748	
	125	1.40	0.93	3.2	13.17	0.914	
	126	1.31	0.91	3.4	12.19	0.864	
	127	1.41	1.00	2.9	13.19	0.857	
	128	1.20	0.82	2.2	11.60	0.907	
	129	1.14	0.92	4.4	12.60	0.875	
+ 0.75	130	1.28	0.77	1.5	10.58	0.879	
	131	0.92	0.86	2.7			*
	132	1.10	0.87	2.0			*
	133	0.96	0.93	3.4	10.18	0.707	
	134	1.11	1.05	1.4			*
	135	1.04	0.79	3.1	10.53	0.853	
	136	0.87	0.78	1.2	9.99	0.820	
	137	0.97	0.77	2.7			*

TABLE 1 - (Continued)

ϕ size	NO.	D_l (mm)	D_i (mm)	ρ_r	W_m (cm/sec)	W_m / W_s	
+ 0.75	138	1.08	0.84	1.3	10.13	0.774	
	139	0.97	0.84	2.5	9.26	0.707	
	140	1.05	1.00	3.1	10.25	0.666	
	141	1.08	0.79	3.7			*
	142	1.00	0.90	3.1	10.55	0.756	
	143	0.86	0.77	3.4	7.65	0.636	
	144	0.93	0.74	2.2	9.86	0.853	
	145	1.02	0.82	3.1	10.53	0.824	
	146	1.10	0.67	4.2	11.40	1.089	
	147	1.08	0.77	2.2			*
	148	0.96	0.77	4.4	9.57	0.796	
	149	1.11	0.77	2.8	11.55	0.961	
	150	0.95	0.80	2.5	9.60	0.770	
	151	1.11	0.78	2.3	9.83	0.808	
	152	0.92	0.90	1.5	9.43	0.676	
	153	1.02	0.74	2.9	9.89	0.857	
	154	1.18	0.82	2.4	10.58	0.829	
+ 1.00	155	0.98	0.86	2.8	7.89	0.591	
	156	0.77	0.64	2.9	8.51	0.853	
	157	0.82	0.64	1.7	8.18	0.820	
	158	1.02	0.73	2.2	6.41	0.563	
	159	0.96	0.74	2.7	8.44	0.731	
	160	1.00	0.70	4.0	8.71	0.797	
	161	0.67	0.61	4.2	8.22	0.866	
	162	0.84	0.65	2.0	8.29	0.818	
	163	0.96	0.67	1.3	7.39	0.708	
	164	0.90	0.72	0.8	8.51	0.758	
	165	0.80	0.67	2.7	7.97	0.764	
	166	0.80	0.63	3.1	8.26	0.843	
	167	0.95	0.72	1.0	7.78	0.693	
	168	0.93	0.69	1.7			*
	169	0.76	0.55	3.2	9.02	1.062	
	170	0.90	0.64	4.2	8.98	0.902	
	171	0.90	0.60	2.3	7.90	0.848	
	172	0.77	0.56	2.4	8.03	0.928	
	173	0.76	0.66	2.3	8.45	0.822	
	174	0.76	0.59	2.6	9.37	1.024	
	175	0.76	0.67	3.2			*
	176	0.90	0.69	4.2	7.11	0.661	
	177	0.87	0.77	2.6	7.02	0.587	
	178	0.95	0.65	2.3	8.93	0.885	
	179	0.76	0.61	2.8	8.25	0.874	
+ 1.25	180	0.74	0.54	1.1	6.88	0.829	
	181	0.61	0.60	3.5	6.38	0.687	
	182	0.72	0.55	2.7	7.10	0.839	
	183	0.74	0.69	2.1	6.61	0.617	

TABLE 1 - (Continued)

ϕ size	NO.	D_1 (mm)	D_i (mm)	ρ_r	W_m (cm/sec)	W_m / W_s	
+ 1.25	184	0.65	0.53	2.2	5.99	0.737	
	185	0.68	0.51	2.6	6.42	0.824	
	186	0.70	0.61	2.9			*
	187	0.73	0.57	2.8	6.94	0.789	
	188	0.70	0.67	3.2	6.55	0.629	
	189	0.68	0.63	2.3	6.40	0.657	
	190	0.85	0.51	3.1	6.52	0.883	
	191	0.64	0.59	2.4			*
	192	0.63	0.57	2.2	6.47	0.737	
	193	0.69	0.59	3.1	6.52	0.716	
	194	0.74	0.56	2.9	6.84	0.794	
	195	0.61	0.59	3.3	6.18	0.679	
	196	0.60	0.52	2.4	6.50	0.818	
	197	0.69	0.51	3.1	6.74	0.867	
	198	0.78	0.59	2.9	7.10	0.772	
	199	0.59	0.49	4.3	6.65	0.895	
	200	0.87	0.73	2.3	6.52	0.576	
	201	0.69	0.55	2.0	6.83	0.809	
	202	0.79	0.53	2.3	7.39	0.912	
	203	0.73	0.51	0.6	6.71	0.865	
	204	0.68	0.59	3.7	6.45	0.710	
+ 1.50	205	0.56	0.54	2.1	5.65	0.684	
	206	0.69	0.51	1.3	5.54	0.715	
	207	0.74	0.49	2.7	6.23	0.841	
	208	0.60	0.41	3.5			*
	209	0.74	0.46	1.8	5.45	0.791	
	210	0.60	0.36	2.3	5.07	0.983	
	211	0.58	0.49	2.8	4.86	0.656	
	212	0.58	0.44	0.8	5.77	0.880	
	213	0.54	0.49	2.2	5.48	0.740	
	214	0.72	0.38	4.0	5.72	1.038	
	215	0.55	0.47	2.8	5.01	0.709	
	216	0.86	0.44	2.1	6.11	0.932	
	217	0.69	0.49	1.6	6.04	0.815	
	218	0.54	0.51	1.7			*
	219	0.58	0.51	2.9	5.06	0.653	
	220	0.68	0.44	1.5			*
	221	0.51	0.45	2.1	5.24	0.779	
	222	0.59	0.36	2.0	5.36	1.039	
	223	0.56	0.54	2.3	4.92	0.595	
	224	0.59	0.52	1.7	5.48	0.694	
	225	0.61	0.57	2.3	5.33	0.611	
	226	0.64	0.50	2.3	5.49	0.574	
	227	0.70	0.44	2.1	6.06	0.927	
	228	0.69	0.44	4.6	5.15	0.788	
	229	0.68	0.44	2.7	5.30	0.811	

spheres, Gibbs, et al. (1971) showed that errors are only about ±1 to 2% at a 95% confidence level, indicating that only minor errors are involved in measuring settling velocities.

After filling the settling tube with water, 30 hours elapsed before conducting the measurements so as to allow time for the water to reach equilibrium. A thermometer was hung within the tube in order to monitor any temperature variations during the experiment. No convection currents or other water motions were observed during the period of measurements.

In addition to measuring the settling rates of the grains, any irregular motions of the grains were noted. These consisted of large- and small-scale spiral motions and oscillations, as well as particle spinning. Within our present experimental techniques these secondary grain motions could only be noted qualitatively, and no attempt was made to quantify them. It was observed that the larger the grain size, the larger the scale of these secondary motions. In a few cases, the largest particles performed such large oscillations that they hit the wall of the tube and had to be excluded from the analyses. Due to the large inner-diameter of the settling tube, corrections for wall effects are negligible for the small grains (McNown, et al., 1951). In instances where settling grains spent an appreciable time near the cylinder wall, the results were again excluded. Altogether, 33 grains had to be eliminated due to such problems, leaving 196 to be included in the analyses (Table 1).

DATA ANALYSIS

It is well established that sieving does not accurately represent the real dimensions of natural irregular grains (Hatch, 1933; Herdan, 1953; Ludwick and Henderson, 1968). Ellipsoidal-shaped grains tend to drop through the screen openings with their longest axes vertical to the plane of the screen, the intermediate axes approximately fitting into the diagonals of the square screen openings. Ludwick and Henderson (1968) studied the mechanics of sieving statistically, using artificial ellipsoids having different ratios of the longest, intermediate and shortest axes. It was found that when particles of various sizes are mixed and sieved, the distribution of intermediate diameters shows much higher values than the openings of the sieve screens, and the distributions of grains for each sieve size are bell-shaped and broad, and they overlap one another.

These previous findings are largely confirmed by our measurements. Figure 1 plots the intermediate diameters, D_i, of the quartz grains versus the sieve diameter, the data presented in Table 1. The mean values of D_i for each sieve size were determined, and plotted as X's, and the solid curve drawn through them. The two long-dashed curves show the sizes of the sieve diagonals and sides of the square openings. Also plotted, as the short-dashed curve, is the curve fit to the means of the longest grain diameters, D_l, but without plotting the actual data upon which this curve is based. Although few grains were measured for each sieve size, it would appear that the D_i measurements do form bell-shaped distributions about means, with many values of D_i being larger than the diagonals of the sieves. The means of the D_i measurements approximately correspond to the sieve diagonals, being slightly less for the smallest grain sizes, and increasingly smaller with the coarser grains. The mean lengths of the

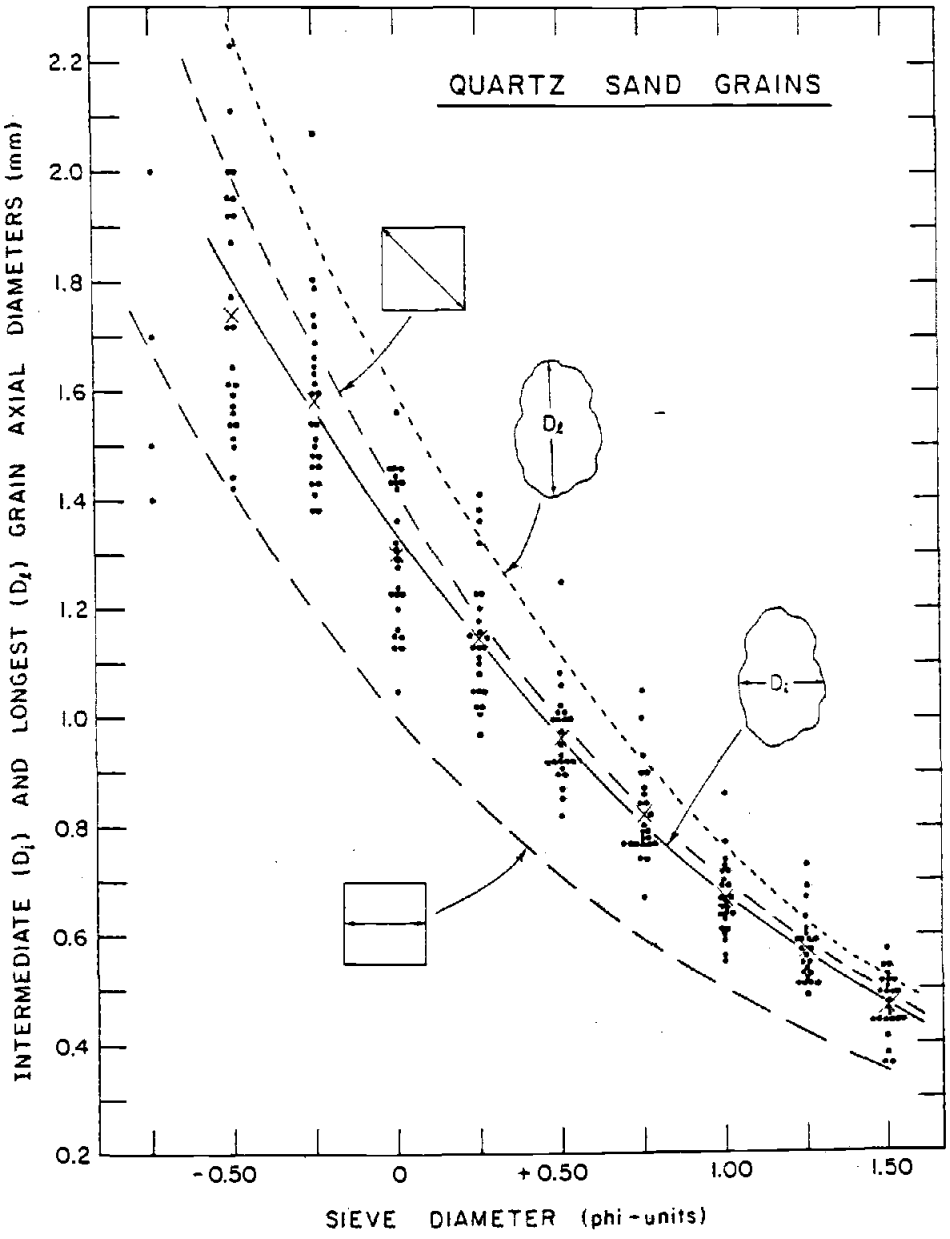

Figure 1: The intermediate diameter D_i versus the sieve diameter for the 229 quartz sand grains. The two long dashed curves are the diagonal and transverse openings of the sieve screens as shown. Also given as the short-dashed curve is the fit to the means of the longest axial diameters, D_l .

longest axial diameter, D_l , are seen to be much larger than the diagonals of the screen openings.

A basic question to be answered in this analysis is what grain-size parameter or dimension do we use in order to obtain the most consistent and accurate prediction of grain settling velocities. We have D_i , D_l and the sieve diameters to choose from since from a practical standpoint, these are most easily measured. Ideally we would like determine the immersed weight of the grain as this most directly relates to the settling velocity, but would obviously be difficult to determine on a routine basis.

With respect to simply plotting the measured settling velocity, w_m , versus the grain size, the intermediate diameter D_i gives the best results when compared with the data of Lane (1938) and the tabulated average values of Mamak (1964). This is shown in Figure 2 where we have plotted our data as w_m versus D_i . This comparison with the previous data sets of settling velocities of natural sand grains is uncertain in that neither Lane (1938) nor Mamak (1964) specified what they took as the grain "diameter". Using D_l rather than D_i shifts our data too far to the right of the other data sets. Using the sieve diameter places our data too far to the left, although it is in closer agreement with the curve for the settling of spheres. As well as not agreeing with the data of Lane and Mamak, plotting our data using the sieve diameter places many of the points above the curve for the settling of spheres, an unlikely position since the irregularities of the natural sand grains can be expected to cause them to settle more slowly than spheres, not faster.

The graph of Figure 2 could be used directly to predict the settling rate of a grain from its measured D_i axial diameter. An alternative and

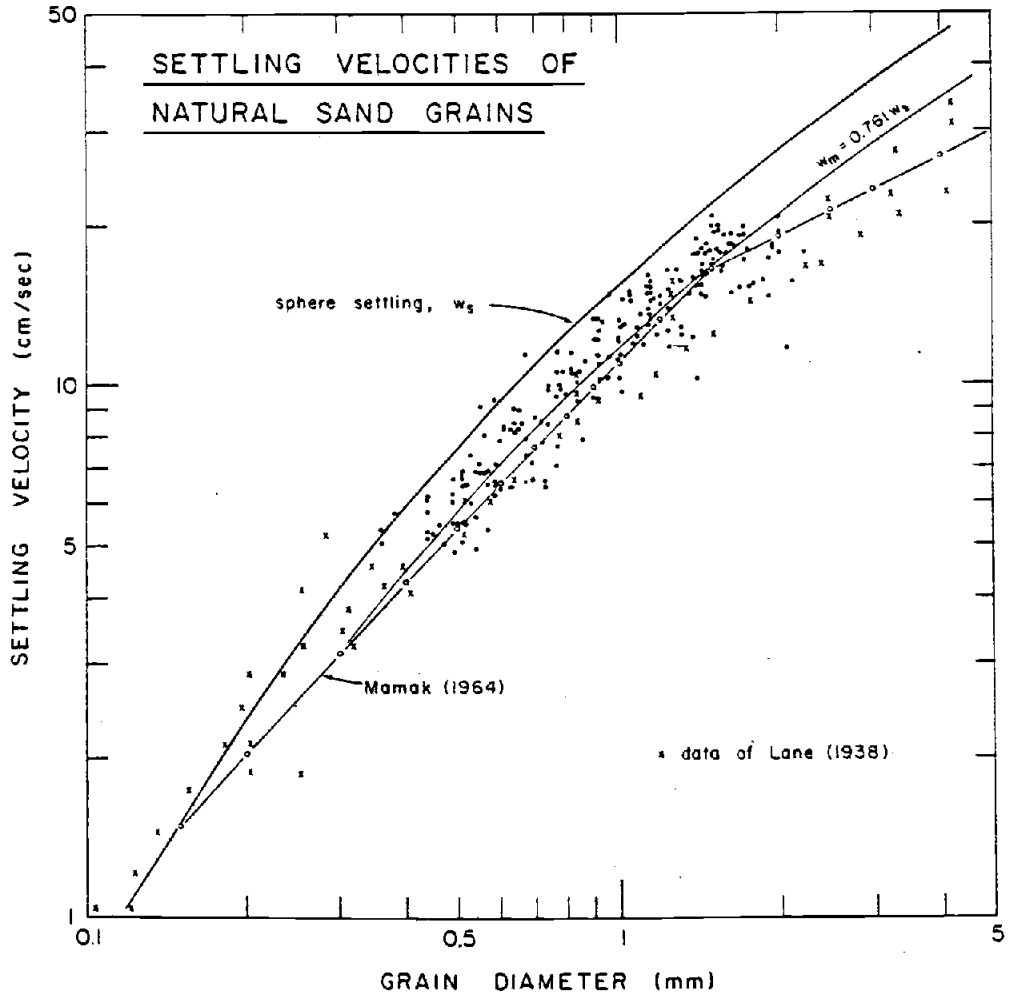

Figure 2: The measured settling velocity versus the grain diameter, taken as D_i for the data of this study. The upper heavy curve is for the settling of spheres.

more accurate approach is to relate the measured settling velocity, w_m, to the settling velocity of the "equivalent sphere", w_s, calculated with the empirical equation of Gibbs, et al. (1971),

$$w_s = \frac{-3\mu + \sqrt{9\mu^2 + gr^2\rho(\rho_s - \rho)(0.015476 + 0.1984|r)}}{\rho(0.011607 + 0.1488|r)} \qquad (1)$$

where μ is the dynamic viscosity of the water in poise units, g is the acceleration of gravity (981 cm/sec^2), ρ is the water density (g/cm^3), ρ_s is the grain density (2.65 g/cm^3 for quartz sand), and r is the sphere radius (cm). This relationship provides a good evaluation for the settling velocities of spheres.

Figure 3 compares the measured settling velocity, w_m, to the settling velocity of a sphere, w_s, calculated with equation (1) using $r = D_i/2$. It is seen that as in Figure 2, w_m is consistently smaller than w_s, progressively departing from the $w_m = w_s$ equivalence as the grain size and settling rates increase. Similar progressive departures are observed in the Lane (1938) and Mamak (1964) data (Figure 2). A linear regression of $\log(w_m)$ versus $\log(w_s)$ yields the relationship

$$w_m = 0.977 w_s^{0.913} \qquad (2)$$

with $R^2 = 0.87$. Equation (2) is plotted in Figure 3 as the dashed curve. We also regressed w_m versus w_s, but the resulting relationship was unsatisfactory. Instead, a straight line was fitted by eye to the data as shown in Figure 3, yielding the equation

$$w_m = 0.761 w_s \qquad (3)$$

This very simple relationship is seen to correspond closely to the curve

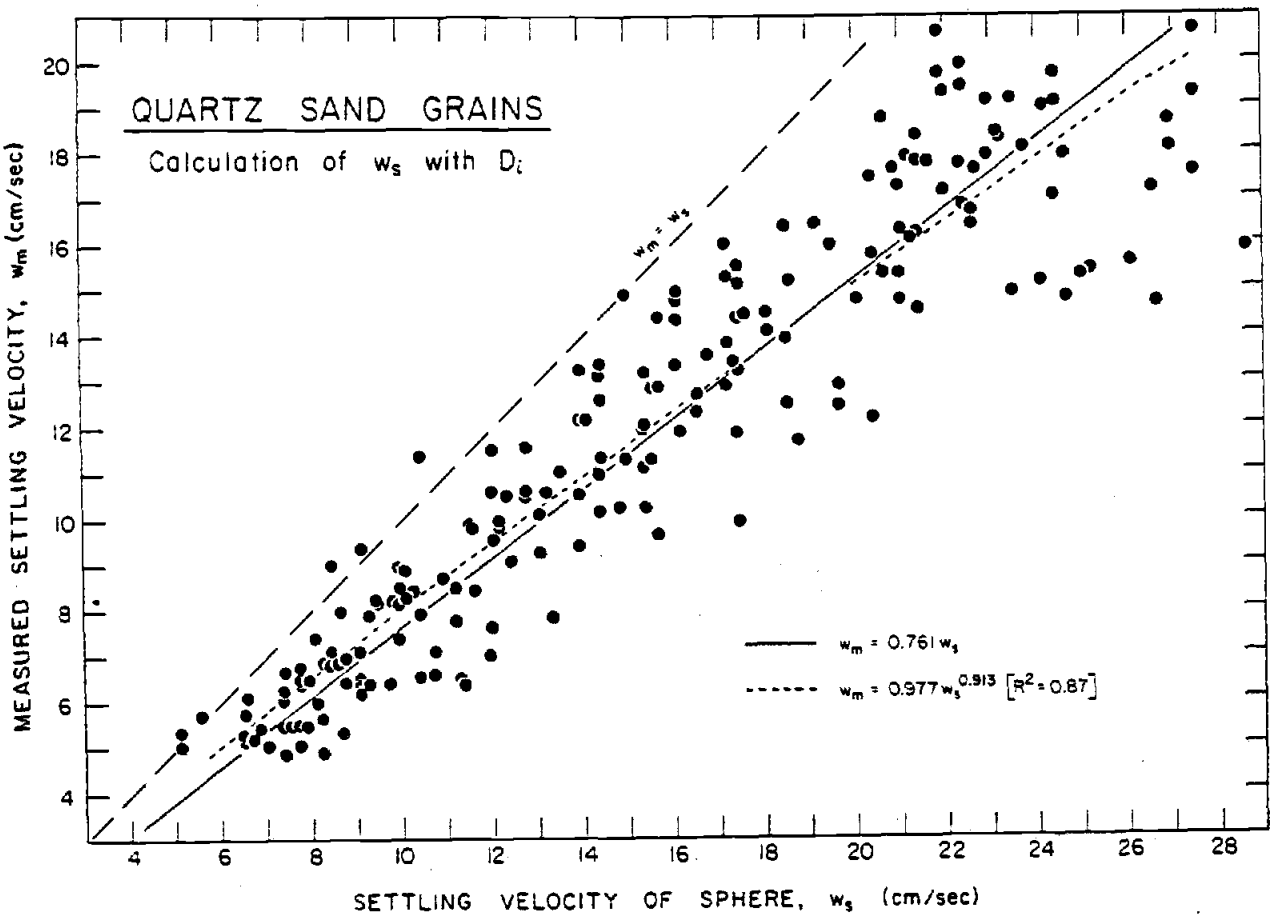

Figure 3: The measured settling velocity, w_m, versus the settling rate of a sphere, w_s, calculated with equation (1) using $r = D_i/2$.

of equation (2) in Figure 3. Equation (3) is also shown in Figure 2 where it is seen to represent a simple downward shift in the settling velocity curve, a 0.761 factor below the curve for the settling of spheres. Equations (2) and (3) obviously provide a very simple means for determining the average settling velocities of natural irregular grains, w_m, from the more easily determined rates for spheres, w_s. Thus from simple measurements of D_i, we can calculate w_s using equation (1), and then estimate what its actual settling velocity will be according to equations (2) or (3).

Although the use of D_i is preferable to the sieve diameter for the relationship to the settling velocity, in some applications we may wish to go straight from a sieve diameter to a settling velocity without making microscopic measurements of D_i. Thus the same procedure to that above was employed, but using the sieve diameter to calculate the sphere settling rates, w_s, of equation (1). This is plotted against the measured rates in Figure 4, similar to Figure 3 where D_i was used. As discussed earlier, using the sieve diameter results in many cases where the predicted w_s is larger than w_m, an unlikely situation. But the curve of Figure 4 does provide a graphical means by which sieve diameters can be equated to settling velocities of the natural grains without assuming they are spherical.

Although the above procedures provide methods for determining settling velocities of natural sand grains, we have as yet not examined the causes of the departure of w_m from w_s. We can be fairly certain that w_m is less than w_s because of the irregularities of the natural grains which caused them to oscillate and spin as observed in the experiments.

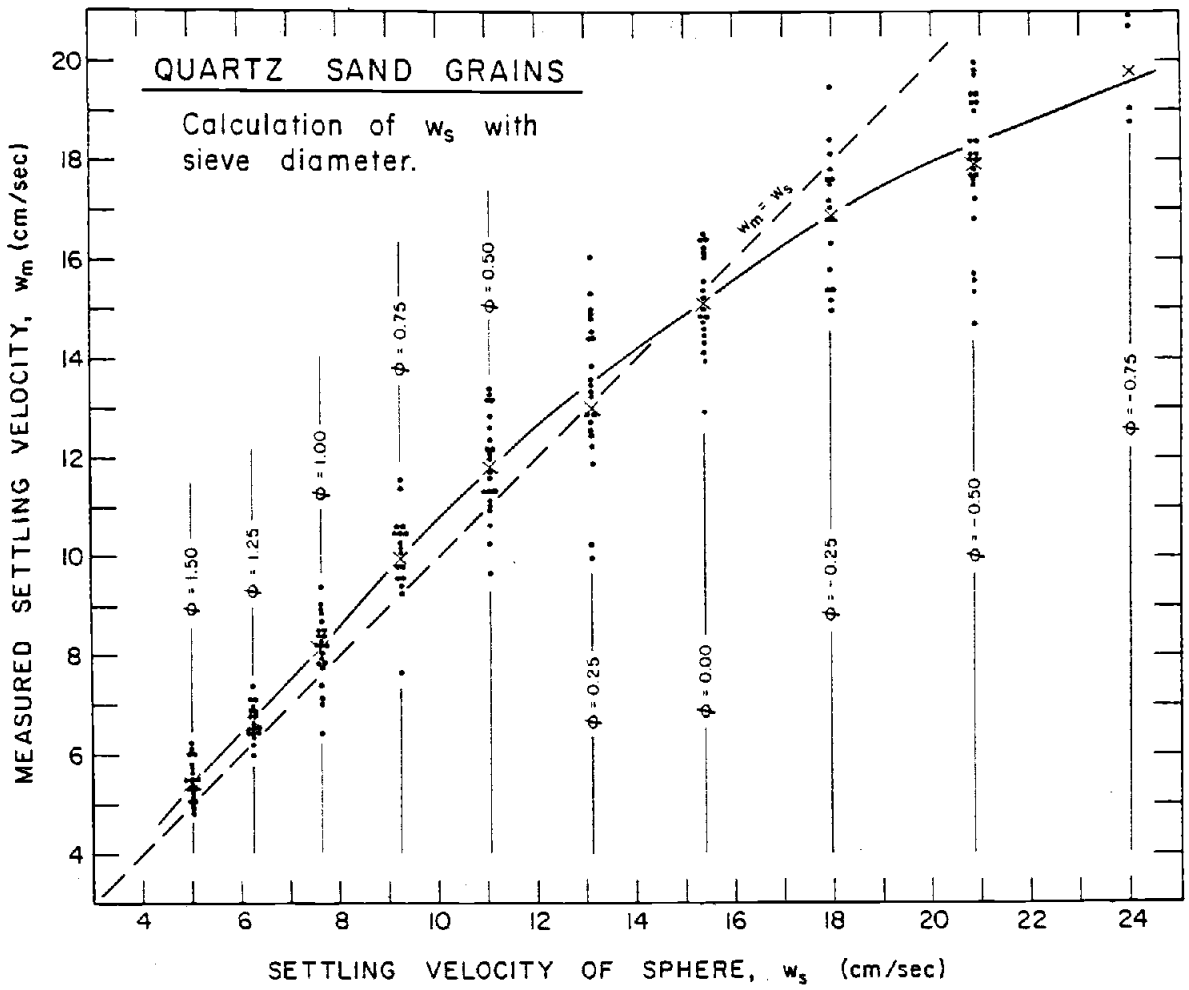

Figure 4: A comparison of the measured settling velocity, w_m, with the settling rate of a sphere calculated with equation (1) using the sieve diameter.

These irregular motions were negligible in the smallest grains settling at the slower rates, and progressively increased in scale with increasing grain diameter. This increase in irregular motions with increasing grain size probably accounts for the progressive departure from the curve of settling of spheres as the grain size increases, seen in the data sets of Lane (1938) and Mamak (1964) as well as in our data (Figure 2).

The possible grain irregularities involved are the degree of grain roundness, sphericity, and grain asymmetries. With the present limitations of our measurements, only grain roundness effects can be examined quantitatively. In Figure 5 we plot our data as grain roundness, ρ_r, versus w_m/w_s, where w_s is calculated with equation (1) using D_i. There appears to be no dependence, supporting the conclusion of Baba and Komar (in press) that grain roundness has no measurable effect on their settling velocities as compared with other effects. Therefore, none of the scatter of our data can be attributed to grain roundness, nor can the result that in nearly all cases $w_m < w_s$ have been caused by increased grain surface drag produced by the grain angularity.

Previous studies of grain shape effects (McNown, et al., 1951; Komar and Reimers, 1978; Komar, 1980) all demonstrate that the non-sphericity of a grain can cause its settling velocity to be smaller than that of an equivalent sphere. The data of those previous studies are generally at lower Reynolds numbers than the present measurements, but the results do indicate that all or nearly all of the reduction in the settling velocity from that of spheres can be accounted for by grain shape effects. At the higher Reynolds numbers of the present experiments, departures from a spherical shape begin to induce the observed oscillations while settling.

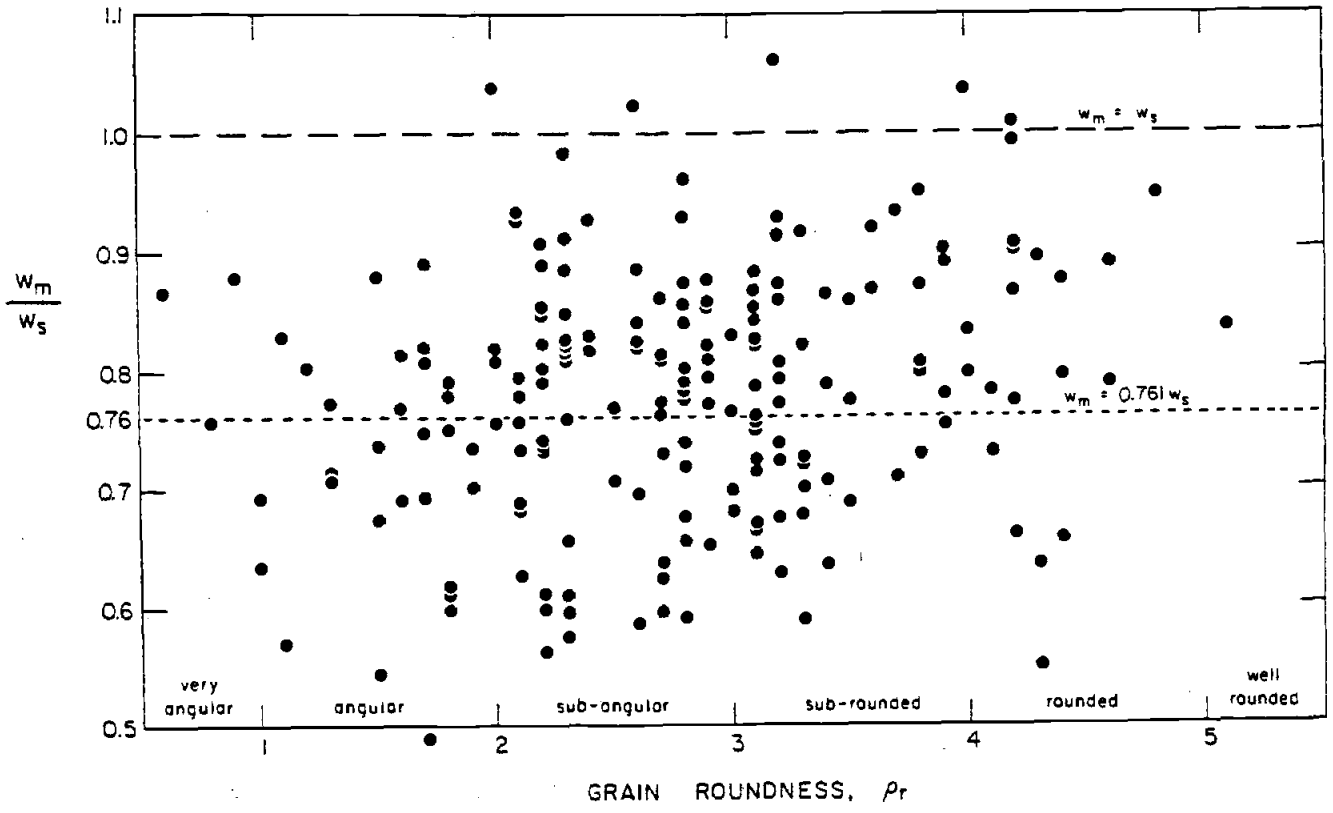

Figure 5: Comparison of the measured settling velocity divided by the calculated settling rate of an "equivalent sphere" with the grain roundness, demonstrating no dependence.

Also important, however, are the grain asymmetries which will cause an imbalance of forces acting on the grains while settling, also inducing them to oscillate and spin. In the present experiments we are unable to distinguish between the effects of grain shape (symmetrical) versus the unsymmetrical irregularities of the natural sand grains. These effects probably also account for the scatter of the data, the more nonspherical or irregular the grain, the greater its reduction in settling velocity from that of a sphere. A range of grain sphericities and irregularities in the sand could thus produce the data scatter seen in Figures 2 through 5. Our above procedures using equations (2) and (3) yield only the average settling rates of the grains, corresponding to an average sphericity and other irregularities found in natural sands.

SUMMARY

The measured settling velocities of natural sand grains are significantly lower than the rates of spheres. This appears to be due to the nonsphericity of the grains and their asymmetries, both of which induce irregular oscillations and grain spinning while settling. Grain roundness was shown to have a negligible effect.

The intermediate diameters of the grains, D_i, showed the most consistent relationship to their settling velocities. An analysis procedure was arrived at wherein either D_i or the sieve diameter can be used in the equation of Gibbs, et al. (1971) to evaluate the settling rate of an "equivalent sphere", and then that value corrected to yield the average settling velocity of the natural sand grains.

ACKNOWLEDGEMENTS

We would like to thank Alan P. Morse for his considerable help in the construction of the settling tube, and for his assistance in conducting the grain settling measurements. Thanks also to Rob Holman for his constructive review of this paper.

REFERENCES

BABA, J. and KOMAR, P.D., in press, Settling velocities of irregular grains at low Reynolds numbers: Jour. of Sed. Petrology.

BLATT, H., MIDDLETON, G., and MURRAY, R., 1972, Origin of Sedimentary Rocks: Prentice-Hall, Inc., Englewood Cliffs, N.J., 634 pp.

FOLK, R.L., 1955, Student error in determination of roundness, sphericity and grain size: Jour. of Sed. Petrology, v. 25, p. 297-301.

FOLK, R.I., 1964, Petrology of Sedimentary Rocks: Hemphill's, The University of Texas, Austin, 154 pp.

GIBBS, R.J., MATTHEWS, M.D., and LINK, D.A., 1971, The relationship between sphere size and settling velocity: Jour. of Sed. Petrology, v. 41, p. 7-18.

GRAF, W.H., and ACAROGLU, E.R., 1966, Settling velocities of natural grains: Bulletin International Assoc. of Sci. Hydrology, v. XI, n. 4, p. 27-43.

HATCH, T., 1933, Determination of "Average Particle Size" from the screen-analysis of non-uniform particulate substances: Jour. Franklin Inst., v. 215, p. 27-37.

HERDAN, G., 1953, Small particle statistics: Elsevier, Amsterdam, 520 pp.

KOMAR, P.D., 1980 , Settling velocities of circular cylinders at low Reynolds numbers: Jour. of Geology, v. 88, p. 327-336.

KOMAR, P.D., and REIMERS, C.E., 1978, Grain shape effects on settling rates: Jour. of Geology, v. 86, p. 193-209.

LANE, E.W., 1938, Notes on the formation of sand: Trans. Amer. Geophys. Union, v. 18, p. 505-508.

LUDWICK, J.C. and HENDERSON, P., 1968, Particle shape and inference of size from sieving: Sedimentology, v. 11, p. 197-235.

MAMAK, W., 1964, River Regulation (Polish), Translation by: U.S. Dept. of Interior and NSF, Washington, D.C.

McNOWN, J.S., and NEWLIN, J., 1951, Drag of spheres in cylindrical boundaries: Proc. 1st National Congress Applied Mechanics.

POWERS, M.C., 1953, A new roundness scale for sedimentary particles: Jour. of Sed. Petrology, v. 23, p. 117-119.